

ORIGINAL RESEARCH ARTICLE

Research on three-dimensional spectrum mapping driven by propagation model

Qiuming Zhu^{1,2*}, Xiaofu Du^{1,2}, Qihui Wu^{1,2}, Jie Wang^{1,2}, Yi Zhao^{1,2}, Kai Mao^{1,2}, Weizhi Zhong^{1,3}

^{*1} Key Laboratory of the Ministry of Industry and Information Technology of Electromagnetic Spectrum Spatial Cognitive Dynamic System, Nanjing University of Aeronautics and Astronautics, Nanjing 211106, China. E-mail: zhuqiuming@nuaa.edu.cn

² School of Electronic Information Engineering, Nanjing University of Aeronautics and Astronautics, Nanjing 211106, China

³ School of Aeronautics and Astronautics, Nanjing University of Aeronautics and Astronautics, Nanjing 211106, China

ABSTRACT

Spectrum map is the foundation of spectrum resource management, security governance and spectrum warfare. Aiming at the problem that the traditional spectrum mapping is limited to two-dimensional space, a three-dimensional spectrum data acquisition and mapping system architecture for the integration of space, sky and earth is presented, and a spectrum map reconstruction scheme driven by propagation model is proposed, which can achieve high-precision three-dimensional spectrum map rendering under the condition of sparse sampling. The spectrum map reconstructed by this method in the case of single radiation source and multiple radiation sources is in good agreement with the theoretical results based on ray tracing method. In addition, the measured results of typical scenes further verify the feasibility of this method.

Keywords: Spectrum Space; Spectrum Situation; Spectrum Map; Spectrum Mapping; Communication Model; Ray Tracing

ARTICLE INFO

Received: 18 March 2022
Accepted: 26 April 2022
Available online: 7 May 2022

COPYRIGHT

Copyright © 2022 by author(s).
Journal of Geography and Cartography is published by EnPress Publisher LLC. This work is licensed under the Creative Commons Attribution-NonCommercial 4.0 International License (CC BY-NC 4.0).
<https://creativecommons.org/licenses/by-nc/4.0/>

1. Introduction

With the advent of 5G era, electromagnetic spectrum has become an indispensable national strategic resource. However, with the rapid development of the integrated information network, the electromagnetic spectrum space is facing the shortage of spectrum resources. The severity of spectrum security and the intensity of spectrum confrontation are also becoming increasingly severe and extending to the airspace. Electromagnetic spectrum includes not only the current state of electromagnetic environment, but also its development trend, so it is also called electromagnetic spectrum situation. The core of spectrum situation research is to map the complex electromagnetic environment into the information space to form a virtual electromagnetic spectrum space.

The electromagnetic spectrum map represents the received signal strength, channel gain, the spatial distribution of radio parameters such as interference power in the region of interest, and the information is visually displayed on the geographical map. Electromagnetic spectrum map, also known as radio environment map (REM), electromagnetic environment map (EEM) and radio frequency radio environment map (RF-REM), etc.^[1,2], can describe the real situation more accurately

because it takes into account the differences in the spatial distribution of the actual electromagnetic environment. Spectrum map reconstruction is also called spectrum mapping. Through the spectrum map, users can intuitively understand the spectrum situation in the measurement area, so as to further analyze and predict the comprehensive situation and future development trend of the spectrum, and finally complete the black broadcast search, base station layout optimization and wireless network interference optimization.

Electromagnetic spectrum mapping is an important part of the current spectrum situation research, including the acquisition of measured values containing geographical location information, and the reconstruction of a complete spectrum map using spatial interpolation or other data processing methods^[3-6]. At present, commercial systems mainly include television white space (TVWS) commercial systems in the United States^[7], the European Union's cognitive radio system measurement and modeling of cognitive radio access system^[8], and TCI's Scorpio Spectrum Monitoring system. In the field of academic research, Guo *et al.*^[9] built a distributed electromagnetic spectrum real-time monitoring system to conduct spectrum mapping. Patino *et al.*^[10] used the sensor that can obtain and record the received signal strength, GPS position information, temperature, humidity and other parameters to build a spectrum mapping system. Melvasalo *et al.*^[11] used distributed radars and RF sensors at different locations to complete data acquisition. Janakaraj *et al.*^[12] obtained campus spectrum situation data throughout the campus through 116 students using handheld spectrum analyzer.

In order to obtain accurate mapping results, a large number of monitoring nodes are needed for the existing spectrum mapping systems, so it is very time-consuming and labor-intensive. In addition, it is limited by the monitoring frequency band, time period, space deployment and other factors, the spectrum data obtained is often sparse, and need to use data processing methods for data reasoning, completion and prediction. At present, the commonly used spectrum data processing methods can be divided into two categories: data-driven and model driven.

The data-driven processing method does not rely on any prior knowledge to estimate the unknown location, but its map reconstruction accuracy is not as good as the model driven processing method. Although the model driven processing method has high accuracy, it needs more theoretical knowledge of radio wave propagation and accurate channel model. In short, the main challenge of current spectrum map reconstruction is how to obtain a high-precision spectrum map with a small amount of sampled data when the emitter information in the measurement area is unknown. In addition, the mapping of spectrum map by the existing system is limited to two-dimensional space, which is difficult to meet the development needs of the future integration of space, sky and ground. The main work of this paper is as follows.

The architecture of electromagnetic spectrum mapping system for the integration of space, sky and earth is given, and the basic characteristics and applicable scenarios of sky-based, space-based and ground-based spectrum mapping systems are introduced, and the existing typical systems are compared.

This paper expounds the spectrum data processing and map reconstruction methods of data-driven and model driven, analyzes and summarizes the applicable scenarios, advantages and disadvantages of these two kinds of reconstruction methods. The data-driven method does not need the prior information of the measurement scenario, and is easy to implement, while the model driven method has high reconstruction accuracy, but it is difficult to be applied in practice.

A three-dimensional spectrum map mapping system based on UAV is developed, and a spectrum map reconstruction scheme driven by propagation model is proposed. The output results are simulated and verified by ray tracing technology, and finally tested in the campus scene.

2. Research status of spectrum mapping

2.1 Spectrum mapping system

The spectrum mapping system can realize the cognition, restructure, storage and visual display of

spectrum situation. The system architecture of electromagnetic spectrum mapping for the integration of sky, space and ground is shown in **Figure 1**. Among them, the spectrum acquisition data is obtained from the satellite constellation, the UAV group and ground monitoring equipment, and transmitted to the spectrum data processing terminal. The terminal performs relevant processing according to the collected spectrum data, and presents the spectrum situation in the measurement area in a visual form.

According to the type of platform carried by the spectrum measurement equipment, the electromagnetic spectrum mapping system can be divided into three types of sky-based, space-based and ground-based. Among them, the sky-based mapping system uses satellites to obtain global spectrum information, and the ground-based mapping system uses the handheld spectrum analyzer, the spectrum monitoring vehicle and other equipment to obtain the ground spectrum information, while the space-based mapping system uses hot-air balloons, helicopter, UAV and other airspace flight equipment to collect airspace spectrum data.

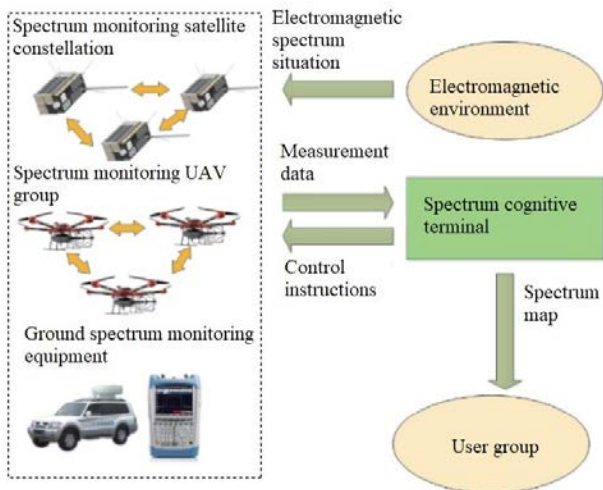


Figure 1. Spectrum mapping scheme based on the integration of space, sky and earth.

Space-based spectrum mapping systems mainly include Kleos Space in France and HawkEye360 in the United States. Among them, Kleos Space provides geographic positioning intelligence data service, and uses VHF signal to locate the ship's position when the automatic identification system is turned off. It is mainly used for maritime situational

awareness. Its monitoring satellite and visualization effect are shown in **Figure 2a**; HawkEye360 realizes high-precision radio mapping and uplink RF signal positioning by collecting specific radio uplink transmission signals around the world. Its monitoring satellites and ground stations are shown in **Figure 2b**.

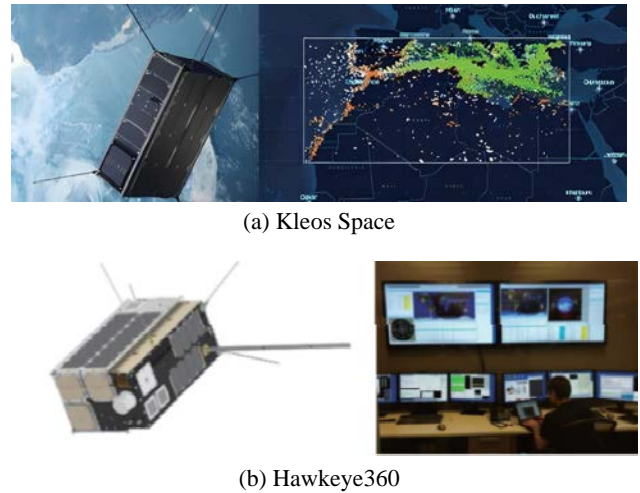


Figure 2. Space-based spectrum mapping system.

At present, there are many ground-based spectrum mapping systems. Among them, most of the ground-based spectrum mapping systems used for scientific research use spectrum sensing sensors or handheld spectrum analyzers arranged in the region of interest, such as R & S © FSH handheld spectrum analyzer of Rohde & Schwarz, as shown in **Figure 3**. The commercial ground-based electromagnetic spectrum mapping system includes the remote spectrum monitoring visualization system MS280001A and MS280007A of Japanese Anli company.



Figure 3. R & S © FSH handheld spectrum analyzer.

A typical commercial space-based electromagnetic spectrum mapping system is the tethered UAV monitoring system Colibrex LS OBSERVER AMU of the German company Colibrex, as shown in **Figure 4**. The system can complete the functions of spectrum map drawing and antenna pattern measurement, but as it is a tethered system, its measurement range is extremely limited. In the field of academic research, Du *et al.*^[6] proposed an airspace spectrum situation mapping system based on UAV platform, which can realize the drawing of air-ground spectrum situation map.



Figure 4. Colibrex LS OBSERVER AMU mapping system.

2.2 Data driven spectrum map reconstruction

2.2.1 Basic principle of data-driven reconstruction method

Data driven spectrum map reconstruction mainly consists of data-driven spectrum completion and spectrum prediction. The implementation principle is shown in **Figure 5**. Spectrum completion method, also known as spatial interpolation construction method or direct construction method, uses known spectrum data to directly estimate the spectrum data at unknown locations^[4], does not need any prior information of physical meaning, and is suitable to show the resource occupation in actual spectrum management.

In addition to the complement based on measured data, it also includes spectrum prediction

technology. Its core idea is to carry out statistical learning for the spectrum data of the past time, analyze and predict the future spectrum situation, so as to achieve the purpose of efficient utilization of spectrum resources^[13].

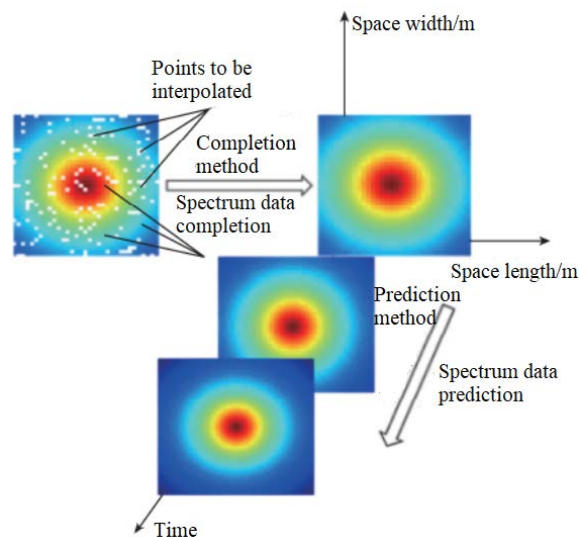


Figure 5. Data-driven spectrum map reconstruction.

2.2.2 Classification of data-driven reconstruction methods

The data-driven reconstruction method estimates the spectrum data of non-sampling positions through spatial interpolation according to the spectrum information of a small number of discrete sampling positions, so as to reconstruct a complete spectrum map. The common classification is shown in **Figure 6**^[14]. Among them, spatial interpolation method can be divided into function interpolation method, spatial geometric interpolation and spatial statistical interpolation.

Function interpolation mainly includes linear interpolation, spline function method and radial basis function method, etc.^[14]. Among them, linear interpolation method and spline function method only considers the spectrum data in the neighborhood, and the reconstruction accuracy and scope of application of both methods are poor. Lazzaro *et al.*^[15] proposed an interpolation method based on radial basis function, which is a combination of a series of accurate interpolation methods and is suitable for high-dimensional space.

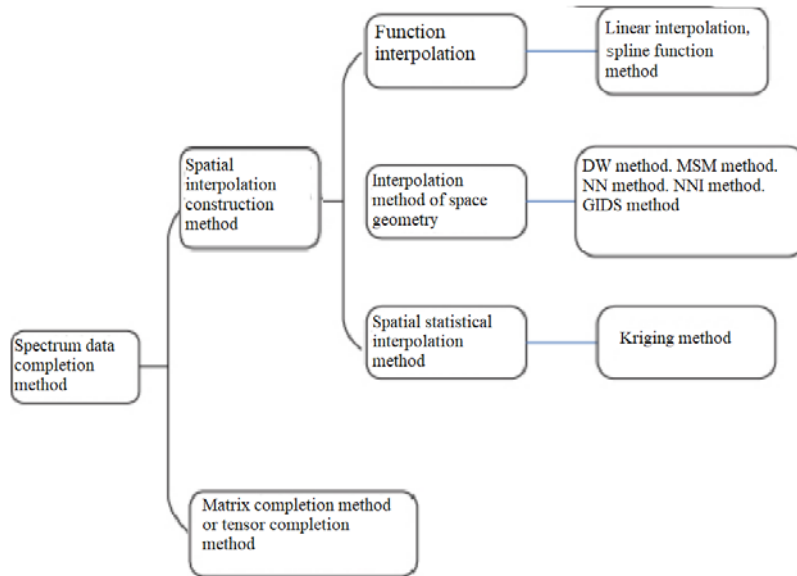


Figure 6. Classification of data-driven completion methods.

Spatial geometry interpolation methods mainly include inverse distance weighted interpolation (IDW) method, modified Shepard's method (MSM), nearest neighbor (NN), natural neighbor interpolation (NNI) and inverse square of gradient distance. Denkovski *et al.*^[16] compared the performance of several interpolation methods based on IDW when the observed values are in different time and space. Zi *et al.*^[17] proposed an improved MSM interpolation algorithm, which can effectively improve the efficiency of the algorithm and has better stability.

Kriging method is a commonly used spatial statistical interpolation method, which requires more monitoring data and complex calculation, but it can give the best linear unbiased estimation, so it has been widely used. Janakaraj *et al.*^[12] proposed an optimal spectrum mapping method based on Kriging method. Zi^[18] used the grid to search the transmitter location, obtaining the location and power estimation of the transmitting node, and combined IDW and Kriging to reconstruct the spectrum map.

For the matrix completion method, Lu^[3] proposed a spectrum map completion method based on the difference of observation values. By combining the difference of sampling point data at the adjacent time to reconstruct the spectrum map at the next time,

the iterative completion mechanism of the spectrum map is realized to ensure the low rank of the matrix to be completed. Cha *et al.*^[19] proposed a nonparametric spectral map reconstruction method, which does not need any specific information such as transmitter and propagation environment, and optimizes the estimated value by using the alternating minimization method according to the monitoring data.

As a high-dimensional expansion of matrix, tensor can better express multidimensional spectrum data. For high-dimensional spectral map reconstruction, Tang *et al.*^[20] extended the low rank of matrix to the low rank of tensor, and proposed a tensor completion method combined with prediction model. Tang *et al.*^[21] used the high-precision low rank tensor completion method to complete the spectrum data. Feng^[22] proposed a low rank tensor decomposition algorithm to solve the complex calculation and noise interference in the tensor completion algorithm.

The spectrum prediction method is based on the past and current spectrum information, and uses the prediction model to analyze and judge the future spectrum state, mainly including the method based on Markov chain, the prediction methods based on regression analysis and neural network, as shown in **Figure 7**.

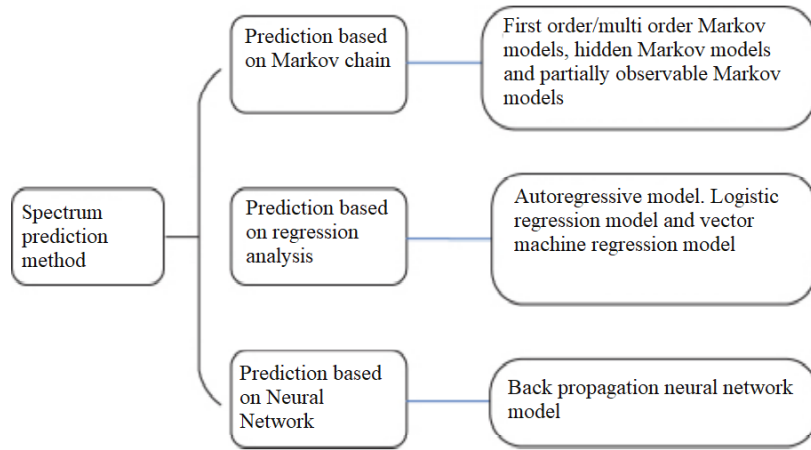


Figure 7. Classification of spectrum prediction method.

The methods based on Markov chain are divided into first-order/multi-order Markov models, hidden Markov model and partially observable Markov model. Federal *et al.*^[23] predicted the channel state through the first-order Markov model. Due to less influencing factors, the prediction performance is general. Zhe *et al.*^[24] used the hidden Markov model to get the connection between data and predict the spectrum state, which has better prediction performance. Zhao *et al.*^[25,26] used some observable Markov models to effectively reduce the conflict between cognitive devices and authorized devices through prediction, considering that the complete spectrum data cannot be perceived in practice.

Regression models are divided into linear regression and nonlinear regression. Linear regression models are generally used to predict continuous data. Wen *et al.*^[27] used a second-order linear autoregressive model to predict and estimate the channel. Gao *et al.*^[28] used the regression model based on vector machine to predict the spectrum data, and compared the prediction performance in different situations through simulation. Jia *et al.*^[29] proposed a spectrum prediction method based on K-nearest neighbor regression, which first predicts the spectrum field strength value, and then improves the model according to the periodicity of the data.

Among the neural network algorithms, the Back Propagation Neural Network (BPNN) model is the most widely used in recent years, and its pattern classification ability is strong. Tumuluru *et al.*^[30] and Yin^[31] studied spectrum prediction using BPNN. Bai

et al.^[32] optimized BPNN based on genetic algorithm and momentum algorithm, making up for its shortcomings of low convergence efficiency and unstable structure.

It should be pointed out that the data-driven reconstruction method is the basis of spectrum map reconstruction, which is simple to implement and has low dependence on specific scene parameters. However, the actual propagation model is not considered. Due to the location of radiation source and other factors, the reconstruction accuracy is low and the predictability is poor.

2.3 Model driven spectrum map reconstruction

Model driven spectral map reconstruction method is also called indirect construction method. Its reconstruction process requires not only monitoring data, but also transmitter information. The basic principle of prior information such as radio wave propagation environment parameters and radio wave propagation model is shown in **Figure 8**. In the field of spectrum mapping, the model in the model driven reconstruction method usually refers to the channel propagation model, so this kind of method also refers to the propagation model driven method. Compared with the data-driven method, due to the introduction of the prior information of the measurement scene, this kind of method has higher reconstruction accuracy than the data-driven map reconstruction method, especially when the number and location of radiation sources in the measurement area are relatively stable,

it can complete the reconstruction and prediction of the electromagnetic spectrum map more accurately, and is more suitable for the situation of sparse

measurement data. Therefore, the model driven method is widely used in coverage monitoring, wireless network planning and other fields.

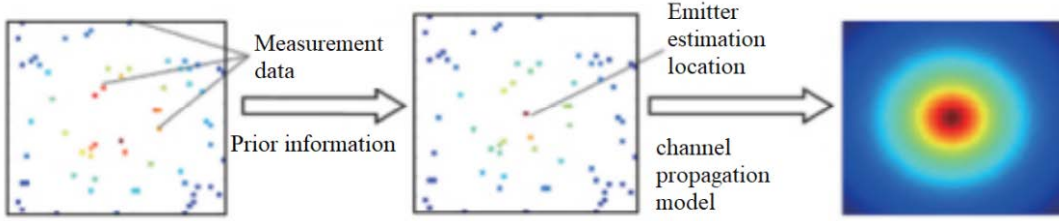


Figure 8. Model-driven spectrum map reconstruction.

There is less research on model driven map reconstruction methods than data-driven methods in the existing literature. Common model driven map reconstruction methods include active transmitter Location Estimation based method (LiVE) and SNR-aided method. These two methods estimate the location and intensity of a single radiation source in the measurement area according to the measurement data and prior information, and obtain the spectrum map of the whole measurement area according to the electromagnetic propagation characteristics. The model driven method similar to the LiVE method and SBR-aided method, as well as the received signal strength difference (RSSD), which application scenario is to measure the emission power of the radiation source in the region. Sato *et al.*^[33] on the basis of LiVE method, combined with Kriging interpolation method, estimated the shadow fading of each position in the measurement area, which improved the performance of spectral map reconstruction.

The above model driven method assumes that there is only one radiation source in the measurement area, which is difficult to be applied in practice. Considering that in actual surveying and mapping, the number of radiation sources in the measurement area is usually unknown, Wang Mengyi *et al.*^[34] combined the traditional IDW method and channel propagation model, gave a reconstruction method that does not need the information of the number of known radiation sources.

3. Model driven spectrum map reasoning and completion

3.1 3D spectrum data acquisition

The typical three-dimensional spectrum mapping scenario is shown in Figure 9, using sky-based or space-based electromagnetic spectrum mapping system. In order to reduce the amount of data to be processed by the reasoning and completion algorithm, it is generally necessary to divide the measurement area. In order to reduce the workload of spectrum data processing, this paper divides the measurement area according to the starting point and end point, and establishes a three-dimensional rectangular coordinate system. Divide the measurement area into $N_1 \times N_2 \times N_3$ cubes, each numbered (n_1, n_2, n_3) , i.e. $((n_1 - 0.5) \times d_1, (n_2 - 0.5) \times d_2, (n_3 - 0.5) \times d_3)$, where d_1, d_2, d_3 respectively represent the length, width and height of each cube. The spectrum data of the whole measurement area is changed from the spectrum matrix of the traditional two-dimensional spectrum map to a third-order spectrum tensor $\chi \in \mathbb{R}^{N_1 \times N_2 \times N_3}$, realizing the modeling of three-dimensional spectrum map data.

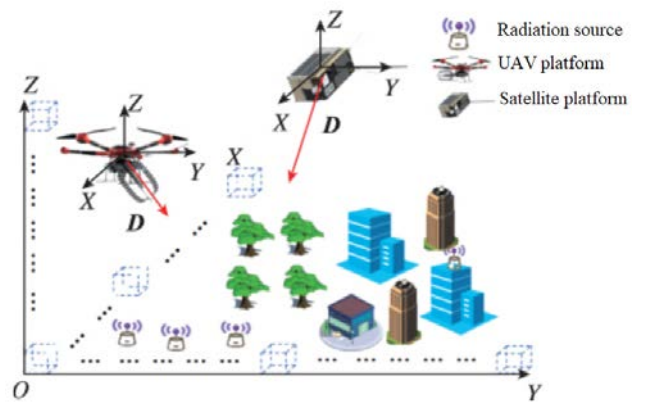


Figure 9. 3D spectrum mapping scheme.

During the surveying and mapping process, the onboard platform first flies according to the test task

and collects spectrum data, and colors the cube at the current position according to the received signal strength. Then, through the model-driven spectral data inference and completion method, the signal strength estimation of other locations in the measurement area is completed, and then a three-dimensional spectral map is constructed.

According to the theory of radio wave propagation, the received signal strength mainly depends on the path loss (PL) and transmit power of all radiation sources in the entire measurement area, and the path loss model is mainly determined by the characteristics of the propagation environment^[35,36]. This paper also considers the effect of log-normal shadow fading on signal strength. Assuming that the received signal strength follows a log-normal distribution, the ideal received signal strength P^{rx} can be expressed as:

$$\begin{aligned} P_i^{rx} &= P_i^{tx} - L_i \\ P_i^{rx} &= 10^{P_i^{tx}/10} \\ P^{rx} &= \sum_{i=1}^{N_{tx}} P_i^{rx} \end{aligned} \quad (1)$$

Where P_i^{tx} is the radiation power of the i -th path, and L_i is the power loss of the i -th path from the radiation source to the cube.

The accuracy of propagation model has a great impact on the performance of model driven spectrum data reasoning and completion methods, so it is very important to select an appropriate propagation model^[37]. The traditional Close-in (CI) model is mainly designed for land mobile communication, without considering the factor of antenna height^[38]. Considering UAV or artificial satellite and other airspace aircraft as the carrying platform, the height of the carrying platform needs to be considered in calculating the path loss^[39]. Therefore, based on the CI model, this paper adds the path loss exponent (PLE) considering the height of the carrying platform. This PL model can be expressed as:

$$\begin{aligned} L(f_c, d, h_{UAV}) [\text{dB}] = & \\ & 32.4 + 20 \log_{10}(f_c) + 10(A + \\ & h_{UAV}^B) \cdot \log_{10}(d) + \chi_\sigma \end{aligned} \quad (2)$$

Where, A and B are the correction parameters

related to the propagation environment, and there is a great difference between the sight distance and non-sight distance scenes; χ_σ is a Gaussian random variable with zero mean, representing the shadow fading factor; d , f_c , h_{UAV} respectively represent the distance, the frequency and the height of UAV. The units are m, GHz and m, respectively.

3.2 Model driven data reasoning

The spectrum data reasoning mechanism is shown in **Figure 11**. When the measuring antenna used is a directional antenna with strong directivity, the received signal strength at each position in the main lobe direction can be obtained from equation (3).

$$P_{(n_1, n_2, n_3)} (\text{dBm}) = P_{UAV} - G_r + L \quad (3)$$

Where, (n_1, n_2, n_3) is the number of the cube passed by the direction vector \mathbf{D} of the directional antenna, P_{UAV} is the received signal strength measured by the UAV at $(X_{UAV}, Y_{UAV}, Z_{UAV})$, G_r is the main lobe gain of the directional antenna, and L is the path loss between the position of the carrying platform and the center point of the cube.

It should be pointed out that the main lobe direction vector of the directional antenna at different positions of the carrying platform may intersect with the same cube. At this time, multi-source spectrum data fusion should be used to determine the final received signal strength of these cubes. Considering that there are multiple radiation sources in the measurement area, when the directional antenna main lobe direction vector measured by the carrying platform at different positions intersects the same cube, it usually indicates that there are radiation sources in the directional antenna main lobe direction at these positions. Therefore, in order to ensure the accuracy of the reasoning value, the received signal strength of these cubes is finally determined by equation (4).

$$\begin{aligned} & P_{(n_1, n_2, n_3), final} \\ & = \sum (P_{(n_1, n_2, n_3) prediction i}, P_{(n_1, n_2, n_3) measure i}) \end{aligned} \quad (4)$$

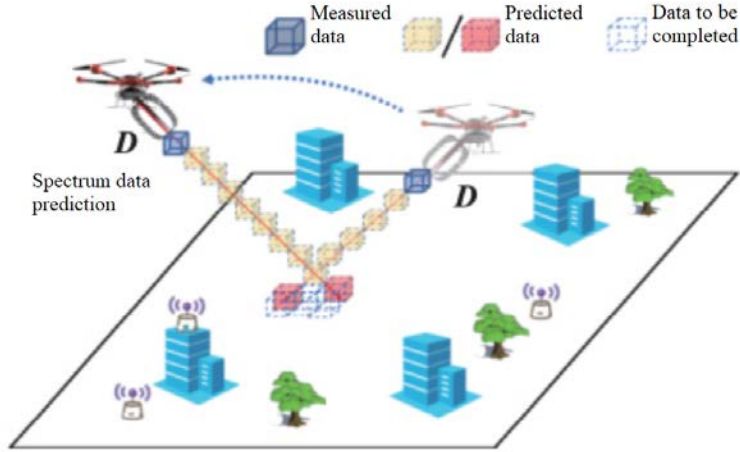


Figure 10. Schematic diagram of spectrum data inference.

In the formula, $P_{(n_1, n_2, n_3), final}$ is finally the received signal strength finally determined by the cube numbered (n_1, n_2, n_3) , $P_{(n_1, n_2, n_3), prediction i}$ is the i -th received signal strength of the cube deduced according to formula (3) when the carrying platform is at different positions, $P_{(n_1, n_2, n_3), measure}$ is the measured value of the carrying platform at the cube (if the carrying platform passes through the cube during measurement). The unit of the above received signal strength is mW.

Compared with the traditional data-driven reconstruction methods (such as IDW method), the propagation model driven three-dimensional spectrum map reconstruction method proposed in this paper adds the step of model driven spectrum data reasoning before data completion, makes full use of the performance advantages of the measurement antenna, and reduces the amount of data that needs to be processed by the data completion algorithm.

3.3 Model driven data completion

After the measurement and reasoning of the received signal strength in the measurement area, the received signal strength of some cubes is unknown. Therefore, it is also necessary to complete the received signal strength of the unknown cube by choosing suitable spectral data completion method.

The classical IDW method believes that the influence of the sampling value of the known point on the estimated value of the unknown point depends on the distance between the sampling point and the unknown point^[40]. In order to get the received signal

strength \hat{P}_{s_0} of the unknown cube s_0 , the IDW method used the last N known cubes s_i , $i = 1, 2, \dots, N$ received signal strengths P_{s_i} , $i = 1, 2, \dots, N$ the weighted average of the N to calculate. Weight ω_i can be calculated by equation (5).

$$\omega_i = \frac{d_i^p}{\sum_{k=1}^N d_k^p} \quad (5)$$

Where, d_i is the distance between s_0 and s_i . Parameter p controls the the decline rate of weight ω_i with distance, p is usually -2 . At this time, the IDW method is called inverse distance square weighting^[41]. Then get \hat{P}_{s_0} according to equation (6).

$$\hat{P}_{s_0} = \sum_{i=1}^N \omega_i P_{s_i} \quad (6)$$

The traditional IDW method only considers the influence of distance and ignores the influence of other factors (such as frequency) in the actual electromagnetic propagation environment on the received signal strength. Considering the characteristics of the propagation environment in the measurement area and combining with the propagation model, the factor affecting the weight is changed into the path loss between the points to be interpolated and the known points. Equation (5) can be rewritten as:

$$\omega_i = \frac{L_i^{-1}}{\sum_{k=1}^N L_k^{-1}} \quad (7)$$

Where L_i represents the path loss between s_0 and

$s_i, i = 1, 2, \dots, N.$

4. Numerical simulation and experimental verification of the algorithm

4.1 Verification test based on RT simulation

4.1.1 Spectrum map RT simulation

In order to verify the effectiveness of the method proposed in this paper, ray tracing (RT) method is used to obtain the spectrum simulation results of the scene to be mapped. RT method is a widely used deterministic channel modeling method. Under the approximate conditions of short wavelength or high frequency, it has excellent accuracy for channel modeling in a small area. RT method is based on geometric optics theory. The principle of uniform diffraction and the superposition theory of field strength track all direct rays, reflection, diffraction and other ray propagation paths in the process of radio wave propagation, and they are used to calculate the propagation parameters such as electric field intensity, amplitude, delay, phase and angle. This paper only focuses on the characteristics of electric field intensity or amplitude.

RT method divides the electric field into sight distance path electric field, reflection path electric field and diffraction path electric field. When there is no obstacle between the transmitting point and the receiving point, its field strength can be expressed as:

$$E_{LoS} = E_0 \frac{e^{-jkd}}{d} \quad (8)$$

Where E_0 is the electric field intensity 1 m away from the transmitting source, k is the wave number, and d is the distance between the transmitting and receiving points.

When obstacles are encountered during propagation, reflection and diffraction will occur. The reflection coefficients of horizontal and vertical polarized waves should be calculated first, and then the field strength should be calculated, which can be expressed as:

$$E_R = E_0 R \frac{e^{-jk(s_1+s_2)}}{s_1 + s_2} \quad (9)$$

$$R_{\parallel} = \frac{\varepsilon \cos \theta - \sqrt{\varepsilon\mu - \sin^2 \theta}}{\varepsilon \cos \theta + \sqrt{\varepsilon\mu - \sin^2 \theta}} \quad (10)$$

$$R_{\perp} = \frac{\cos \theta - \sqrt{\varepsilon\mu - \sin^2 \theta}}{\cos \theta + \sqrt{\varepsilon\mu - \sin^2 \theta}} \quad (11)$$

$$\varepsilon = \varepsilon_r - j60\lambda\sigma \quad (12)$$

Where, θ is the angle of incidence, ε represents the relative dielectric constant of the environment, μ is the relative permeability of the environment, σ is the conductivity of the environment, s_1 is the distance between the transmitting point and the reflecting point or diffraction point, s_2 is the receiving point, R is the reflection coefficient, D is the diffraction coefficient. The diffraction field intensity can be expressed as:

$$E_D = \frac{E_0}{s_1} D \sqrt{\frac{s_1}{(s_1 + s_2)s_1}} e^{-jk(s_1+s_2)} \quad (13)$$

Finally, add the field strength vectors that contribute to the receiving point, and the total field strength of the receiving point is:

$$E_{\text{total}} = \sum_i E_i \quad (14)$$

PL is the ratio of transmit power to receive power, so it can be expressed as

$$PL(\text{dB}) = 20 \lg \frac{E_r}{E_t} \quad (15)$$

Where, E_t is the electric field strength at 1 m, and E_r is the sum of the field strength vectors of the effectively received rays.

When using RT method to calculate the path loss, it is necessary to obtain the details of transmission, receiver location and overall propagation environment. The RT spectrum data acquisition method based on digital map is shown in **Figure 11**, which mainly includes two steps: propagation scene reconstruction and path loss calculation. After obtaining the path loss of different transmitters and receivers, the received signal strength at different locations can be obtained according to the known transmitter power, so as to build the spectrum situation map.

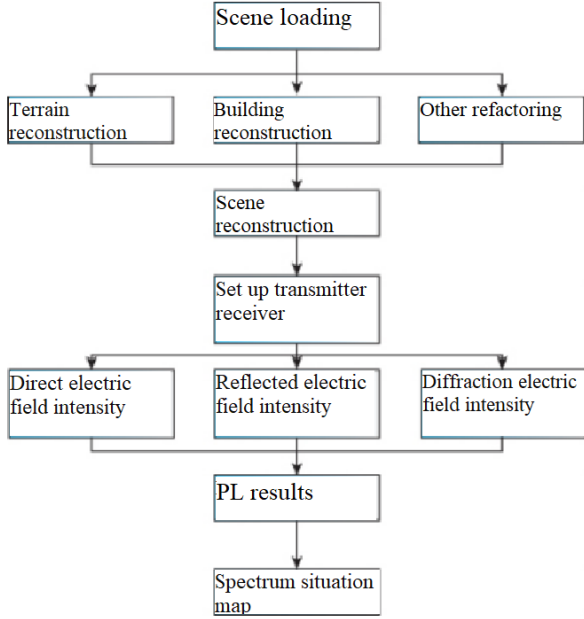


Figure 11. RT simulation method of spectrum map.



(a) Satellite map



(b) Reconstruction map

Figure 12. Campus scenario map.

The scene of Jiangning campus of Nanjing University of Aeronautics and Astronautics is simulated, which includes typical propagation characteristics, such as buildings, woods, vegetation and lakes. The

satellite map and reconstructed digital map of the simulation area are shown in **Figure 12**.

The scene includes 65 buildings, with a minimum height of 19 m and a maximum height of 70 m, an average height of 30 m, and the area of the entire measurement area of $1 \text{ km} \times 1 \text{ km}$. The specific simulation parameters are: the center frequency of the transmitter is 98 MHz, the transmission power is 43 dBm, and it is placed about 2 m away from the ground. Among them, the transmitter is set in three typical positions, which are respectively in the center of the playground, above the water surface and in the middle of the square surrounded by high buildings. The reasoning and completion of the actual spectrum data are three-dimensional data, but in order to facilitate visual display, a 30 m high two-dimensional spectrum map slice is finally given.

4.1.2 Single emitter simulation test

Assuming a single emitter and the emitter is located at TX1 in **Figure 12b**, **Figure 13a** shows the spectrum map obtained by RT simulation method. In order to verify the effectiveness of the data completion method proposed in this paper in the case of a single emitter, the spectrum map with 50% random missing data is used for completion, as shown in **Figure 13b**.

Figure 13c shows the spectrum map after the spectrum map reconstruction method is completed. By comparing **Figure 13a** and **Figure 13c**, it can be seen that the reconstructed spectrum map is in good agreement with the theoretical results obtained by the ray tracing method. Therefore, the map reconstruction performance of the method proposed in this paper is very good in the single emitter scene.

4.1.3 Multi emitter simulation test

For the case of multiple radiation sources, it is assumed that three radiation sources are located at positions of TX1, TX2 and TX3 in **Figure 12b**. The spectrum map construction performance of the proposed data completion method in the case of multiple radiation sources is shown in **Figure 14**, where **Figure 14a** is the spectrum map obtained from RT data, **Figure 14b** is the spectrum map after 50% data loss, and **Figure 14c** is the spectrum map after the completion of the proposed model driven spectrum map

reconstruction method. By comparing **Figure 14a** and **14c**, it can be seen that the reconstructed spectrum map is in good agreement with the theoretical results obtained by the ray tracing method. Therefore, the map reconstruction performance of the method proposed in this paper is very good in the multi emitter scene.

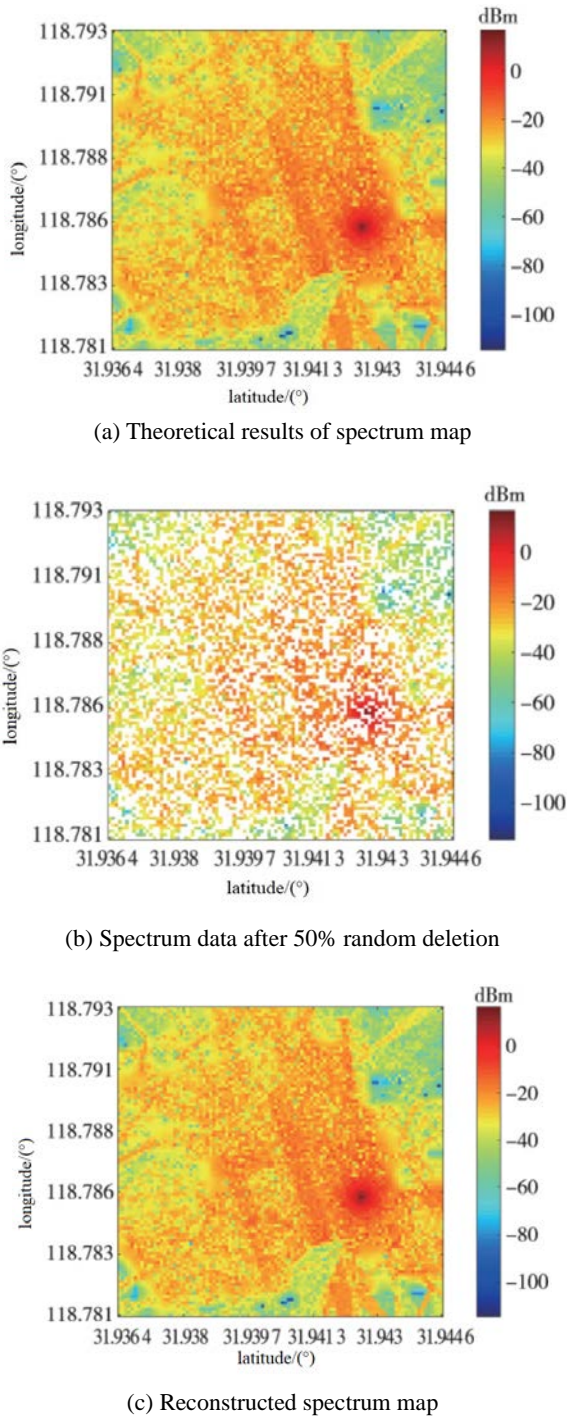


Figure 13. Spectrum map reconstruction with single radiation source.

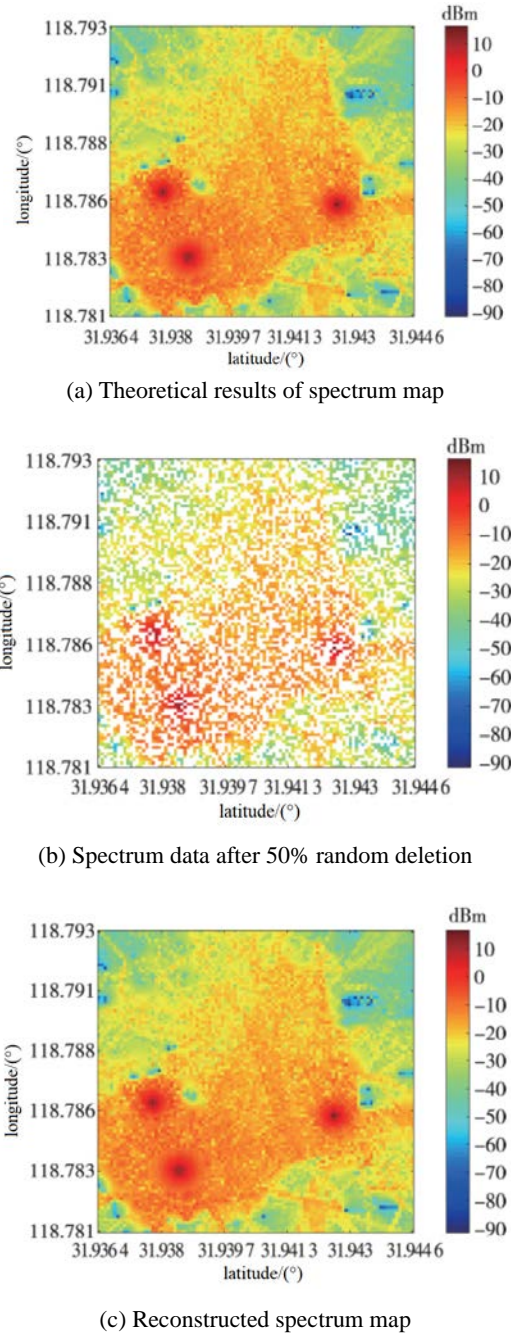


Figure 14. Spectrum map reconstruction with multiple radiation sources.

4.2 Campus scene measurement and analysis

In the early stage, a set of airspace spectrum situation mapping system based on UAV platform was developed. Its system structure is shown in **Figure 15**, and the relevant performance parameters are shown in **Table 1**, mainly including UAV platform subsystem, spectrum monitoring subsystem and ground terminal subsystem. The aerial platform is connected with a high-performance spectrum monitoring subsystem, which is equipped with an omni-

directional antenna for measurement. The directional antenna and the PTZ supporting the directional antenna can collect spectrum information and other information (such as geographical location information) in real time and transmit it to the ground terminal subsystem through the airborne data link module. The ground terminal subsystem can process the spectrum data driven by the channel model for the collected information, and construct the spectrum map of the measurement area.

Table 1. Performance parameters of the system

Index	Numerical value
Monitoring scope	9 KHz ~ 8 GHz
Frequency resolution	1 Hz
Sensitivity	-155 dBm
UAV horizontal speed	26 m/s
UAV vertical speed	8 m/s

As shown in **Figure 16**, the spectrum situation mapping system based on the UAV platform is used for the actual test. The measured area is consistent with the simulation environment, but the emitter information is unknown. After the UAV platform completes the flight path as shown in **Figure 16b**, the proposed model driven spectrum data reasoning and completion algorithm is used to reconstruct the measured data, and finally a complete spectrum map of the measured area is obtained, as shown in **Figure 16**.

Comparing the measured results in **Figure 17** with the geographical map in **Figure 16b**, it can be seen that the received signal intensity near the teaching building in Jiangjun Road Campus of Nanjing University of Aeronautics and Astronautics is the largest, so it can be inferred that there is a radiation source in the broadcast frequency band at this location, which is also consistent with the actual investigation. In addition, the received signal strength in the north of the teaching building is low, and the received signal strength in the south is high. The reason may be that there are other teaching buildings in the north of the teaching building, while the south area is open and the transmission loss is small.

5. Conclusion

High precision spectrum map is an important prerequisite for spatial cognition and control of

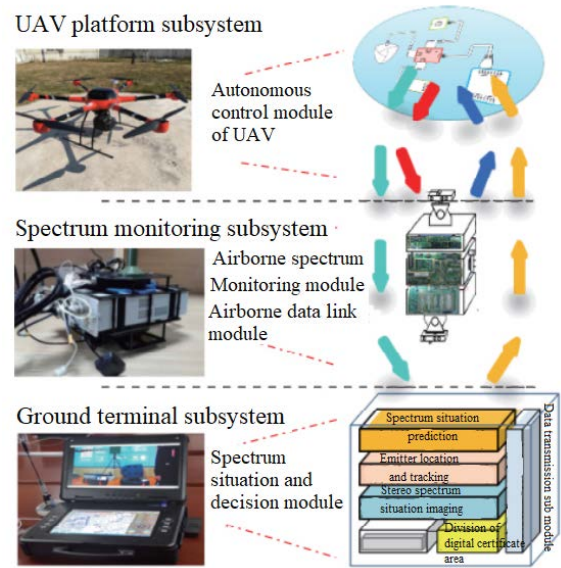


Figure 15. Spectrum mapping system structure.



(a) Measured equipment



(b) Test path

Figure 16. Measurement in the campus scenario.

electromagnetic spectrum. How to reconstruct spectrum map from a small amount of sampled spectrum data is an important problem faced by current spectrum map mapping. This paper proposes a propagation model driven spectrum map reconstruction scheme, including three-dimensional spectrum data acquisition and spectrum data reasoning. The

spectrum map obtained based on this scheme is in good agreement with RT simulation results, and is also consistent with the actual test results of real campus scenes.

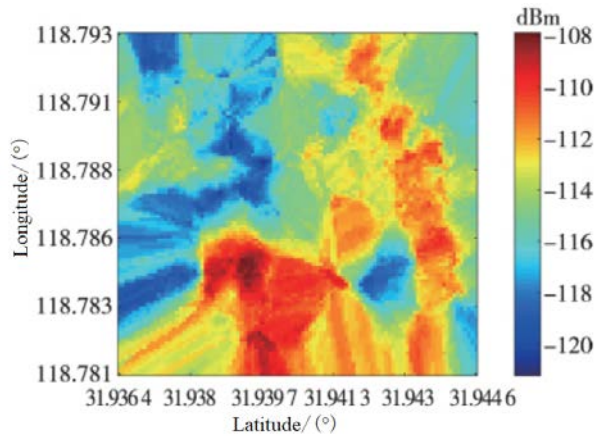


Figure 17. Measured result.

Conflict of interest

The authors declare that they have no conflict of interest.

References

- Ran Z, Chang J, Rong Z, *et al.* Research on the construction of radio environment map based on revised spatial interpolation. *Application of Electronic Technique* 2018; 237: 405–415.
- Hu Y, Zhang R. Differentially-private incentive mechanism for crowd sourced radio environment map construction. *IEEE Conference on Computer Communications*; 2019 Apr 29–May 2; Paris. 2019. p. 1594–1602.
- Lu J. Research on spectral map reconstruction algorithm under incomplete observation conditions (in Chinese) [MSc thesis]. Changsha: National Defense University; 2018.
- Xia H, Cha S, Huang J, *et al.* Review and prospect of electromagnetic spectrum map construction methods (in Chinese). *Chinese Journal of Radio Science* 2020; 35(4): 445–456.
- Lu J, Cha S, Huang J, *et al.* A method to complete the spectrum map based on the difference of observed values (in Chinese). *Journal of Microwaves* 2018; 34 (S2): 426–430.
- Du X, Zhu M, Wu Q, *et al.* UAV-assisted spectrum mapping system based on tensor completion scheme. *MILICOM 2020: Machine Learning and Intelligent Communications*. Cham: Springer; 2020. p. 16–26.
- Bourdena A, Pallis E, Kormentzas G, *et al.* Real-time TVWS trading based on a centralized CR network architecture. *IEEE International Work-shop on Recent Advances in Cognitive Communications and Networking*; 2011 Dec 5–9; Houston. 2011. p. 964–969.
- European Commission. Flexible and spectrum-aware radio access through measurements and modelling in cognitive radio systems. 2020.
- Guo X, Zhang Y, Chen Z, *et al.* Distributed electromagnetic spectrum detection system based on self-organizing network. *12th International Symposium on Antennas, Propagation and EM Theory (ISAPE)*; 2018 Dec 3–6; Hangzhou. 2018. p. 1–5.
- Patino M, Vega F. Model for measurement of radio environment maps and location of white spaces for cognitive radio deployment. *IEEE-APS Topical Conference on Antennas and Propagation in Wireless Communications (APWC)*; 2018 Sep 10–14; Cartagena 2018. p. 913–915.
- Melvasalo M, Koivunen V, Lundn J. Spectrum maps for cognition and co-existence of communication and radar systems. *50th Asilomar Conference on Signals, Systems and Computers*; 2016 Nov 6–9; Pacific Grove. 2016. p. 58–63.
- Janakaraj P, Wang P, Chen Z. Towards cloud-based crowd-augmented spectrum mapping for dynamic spectrum access. *International Conference on Computer Communication and Networks*; 2016 Aug 1–4; Waikoloa. 2016. p. 1–7.
- Hou F. Research on spectrum prediction technology in cognitive radio networks (in Chinese) [MSc thesis]. Beijing: Beijing University of Posts and Telecommunications; 2017.
- Guo Y, Shao W, Zhang Y, *et al.* A hybrid interpolation and extrapolation method for dynamic electromagnetic environment map construction (in Chinese). *Audio Engineering* 2020; 44(10): 72–76.
- Lazzaro D, Montefusco L. Radial basis functions for the multivariate interpolation of large scattered data sets. *Journal of Computational and Applied Mathematics* 2002; 40(1): 521–536.
- Denkovski D, Atanasovski V, Gavrilovska L, *et al.* Reliability of a radio environment map: Case of spatial interpolation techniques. *7th International ICST Conference on Cognitive Radio Oriented Wireless Networks and Communications (CROWNCOM)*; 2012 Jun 18–20; Stockholm. 2012. p. 248–253.
- Zi R, Chang J, Zong R, *et al.* Radio environment map generation technology based on improved spatial interpolation (in Chinese). *Application of Electronic Technique* 2018; 44(3): 103–107.
- Zi R. Research on the construction method of radio environment map (in Chinese) [MSc thesis]. Kunming: Yunnan University; 2018.
- Cha S, Lu J, Huang J, *et al.* Nonparametric spectrum map construction method based on monitoring data (in Chinese). *Journal of Microwaves* 2018; 34(S2): 431–434.
- Tang M, Ding G, Wu Q, *et al.* A joint tensor completion and prediction scheme for multi-dimensional spectrum map construction. *IEEE Access* 2016; 4: 8044–8052.

21. Tang M, Ding G, Zhen X, *et al.* Multi-dimensional spectrum map construction: A tensor perspective. 8th International Conference on Wireless Communications & Signal Processing (WCSP); 2016 Oct 13–15; Yangzhou. 2016. p. 1–5.
22. Feng Q. Research on cooperative spectrum sensing algorithm of cognitive radio system based on tensor analysis (in Chinese) [MSc thesis]. Jilin: Jilin Institute of Chemical Technology; 2020.
23. Federal Communications Commission. Spectrum policy task force. Rep ET Docket No.02–135. Washington: FCC; 2002.
24. Zhe C, Qiu R. Prediction of channel state for cognitive radio using higher-order hidden Markov model. Proceedings of the IEEE SoutheastCon 2010 (SoutheastCon); 2010 Mar 18–21; Concord. 2010. p. 276–282.
25. Zhao Q, Lang T, Swami A, *et al.* Decentralized cognitive MAC for opportunistic spectrum access in ad hoc networks: A POMDP framework. IEEE Journal on Selected Areas in Communications 2007; 25(3): 589–600.
26. Zhao Q, Lang T, Swami A. Decentralized cognitive mac for dynamic spectrum access. First IEEE International Symposium on New Frontiers in Dynamic Spectrum Access Networks; 2005 Nov 8–11; Baltimore. 2005. p.224–232.
27. Wen Z, Tao L, Xiang W, *et al.* Autoregressive spectrum hole prediction model for cognitive radio systems. IEEE International Conference on Communications Workshops; 2008 May 19–23; Beijing. 2008. p. 154–157.
28. Gao X, Ren G, Chen J, *et al.* Spectrum prediction based on support vector regression in fast changing channel environment (in Chinese). Journal of Signal Processing 2014; 30(3): 289–297
29. Jia Y, Qiu L, Wei H. Spectrum occupancy prediction based on K-nearest neighbor regression (in Chinese). Telecommunication Engineering 2016; 56(8): 844–849.
30. Tumuluru VK, Wang P, Niyato D. A neural network-based spectrum prediction scheme for cognitive radio. IEEE International Conference on Communications; 2010 May 23–27; Cape Town. 2010. p. 1–5.
31. Yin L, Yin SX, Hong W, *et al.* Spectrum behavior learning in cognitive radio based on artificial neural network. MILCOM 2011 Military Communications Conference; 2011 Nov 7–10; Baltimore. 2011. p. 25–30.
32. Bai S, Zhou X, Xu F. Spectrum prediction based on improved-back-propagation neural networks. 11th International Conference on Natural Computation (ICNC); 2015 Aug 15–17; Zhangjiajie. 2015. p. 1006–1011.
33. Sato K, Inage K, Fujii T. Radio environment map construction with joint space-frequency interpolation. 2020 International Conference on Artificial Intelligence in Information and Communication (ICAIIIC); 2020 Feb 19–21; Fukuoka. 2020. p. 51–54.
34. Wang M, Sheng Y, Huang Y, *et al.* Spatial interpolation method of electromagnetic geographical environment monitoring data (in Chinese). Journal of Geo-information Science 2017; 19(7): 872–879.
35. Yilmaz HB, Tugcu T. Location estimation-based radio environment map construction in fading channels. Wireless Communications & Mobile Computing 2015; 15(3): 561–570.
36. Zhu MQ, Dang XY, Xu DZ, *et al.* High efficient rejection method for generating Nakagamim sequences. Electronic Letter 2011; 47(19): 1100–1101.
37. Gajewski P. Propagation models in radio environment map design. 2018 Baltic URSI Symposium (URSI); 2018 May 15–17; Poznan. 2018. p. 234–237.
38. Zhu Q, Wang Y, Jiang K, *et al.* 3D non-stationary geometry-based multi-input multi-output channel model for UAV-ground communication systems. IET Microwaves, Antennas & Propagation 2019; 13(8): 1104–1112.
39. Yao M, Chen X, Wang J, *et al.* Ray tracing-based path loss modeling for UAV-to-ground mmWave channels in campus scenario. MILICOM 2020: Machine Learning and Intelligent Communications Engineering. 2020. p. 459–470.
40. Shepard D. A two-dimensional interpolation function for irregularly-spaced data. The 23rd ACM National Conference; 1968 Jan; New York. 1968. p. 517–524.
41. Azpurua MA, Ramos KD. A comparison of spatial interpolation methods for estimation of average electromagnetic field magnitude. Progress in Electromagnetics Research M 2010; 14: 135–145.